Thermal Deligation of $Mo_6S_8L_6$ Cluster Complexes. EXAFS and Other Spectroscopic Techniques Support Retention of the Mo_6S_8 Cluster Unit up to 500 °C

Shane J. Hilsenbeck and Robert E. McCarley*

Ames Laboratory, USDOE, and Department of Chemistry, Iowa State University, Ames, Iowa 50011

Alan I. Goldman*

Ames Laboratory, USDOE, and Department of Physics and Astronomy, Iowa State University, Ames, Iowa 50011

Received August 22, 1994. Revised Manuscript Received January 9, 1995[⊗]

Thermal deligation reactions of N-ligated $Mo_6S_8L_6$ cluster complexes (L = propylamine, pyrrolidine, and piperidine) have been explored at a variety of temperatures in an attempt to form the Mo_6S_8 binary Chevrel phase. Direct heating of the cluster complexes (100–500 °C) under dynamic vacuum has led to varying degrees of ligand removal while retaining the Mo_6S_8 cluster unit in amorphous products. Support for the presence of the cluster unit has been gained by the characteristic Raman band at 445–450 cm^{-1}, XPS data, and results of a Mo EXAFS study. Mo–Mo and Mo–S bond distances derived from the fitting of the EXAFS data for the amorphous products are in good agreement with those for crystalline Mo_6S_8 and $Mo_6S_8L_6$ complexes with well-determined structures. Both XPS and EXAFS show that disproportionation to MoS_2 and Mo does not occur during deligation below 500 °C.

Introduction

Ternary molybdenum chalcogenides of the general formula $M_xMo_6Y_8$ (M = ternary metal cation; Y = chalcogenide; $1 \leq x \leq 4$), known as Chevrel phases, have been extensively studied and shown to include superconductors with high H_{c2},[1] ordered magnetic phases,[2] solid electrolytes (fast ion conductors),[3] and hydrodesulfurization (HDS) catalysts.[4] These properties are related to the structures of the compounds which consist of Mo_6Y_8 clusters interlinked to form three-dimensional networks. The production of the Chevrel phases has generally involved solid state reactions at high temperatures (1000–1300 °C). Yet, lower temperature routes via solution precursors have been sought so that films, coatings, and small particles, either alone or on typical catalyst support materials, can be prepared.[5] We[6,7] and others[8] have recently reported on the preparation of $M_6S_8L_6$ (M = Mo, W) cluster complexes as low-temperature precursors to the Chevrel phases. Figure 1 shows the hexanuclear $Mo_6S_8L_6$ unit where L is an organic ligand for the isolated clusters and a chalcogenide from an adjoining cluster for the Chevrel phases.

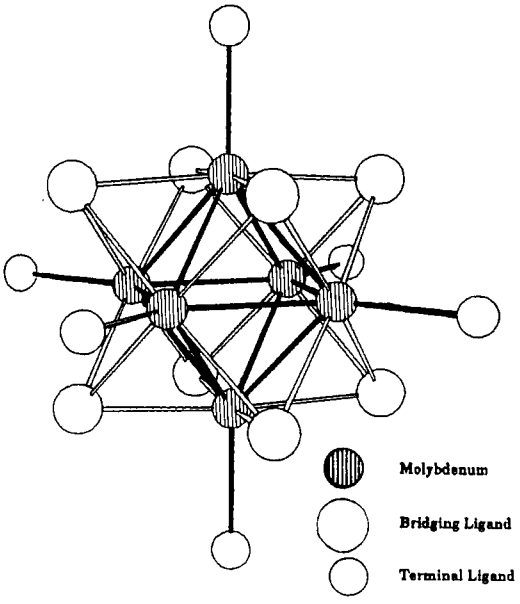

Figure 1. Structure of the $Mo_6Y_8L_6$ cluster unit.

Previous attempts at deligation of the $M_6S_8L_6$ cluster complexes have been explored for the triethylphosphine adduct of the molybdenum complex[9] and the pyridine adduct of the tungsten analogue.[10] For the tri-

[⊗] Abstract published in *Advance ACS Abstracts,* February 15, 1995.

(1) Chevrel, R.; Sergent, M. *Topics in Current Physics,* Fischer, Ø., Maple, M. B., Eds.; Springer-Verlag: Heidelberg, 1982; Vol. 32, Chapter 2.

(2) Peña, O.; Sergent, M. *Prog. Solid State Chem.* **1989,** *19,* 165.

(3) Mulhern, P. J.; Haering, R. R. *Can. J. Phys.* **1984,** *62,* 527.

(4) (a) McCarty, K. F.; Schrader, G. L. *Ind. Eng. Chem. Prod. Res. Dev.* **1984,** *23,* 519. (b) McCarty, K. F.; Anderegg, J. W.; Schrader, G. L. *J. Catal.* **1985,** *93,* 375.

(5) (a) Nanjundaswamy, K. S.; Vasanthacharya, N. Y.; Gopalakrishnan, J.; Rao, C. N. R. *Inorg. Chem.* **1987,** *26,* 4286. (b) Rabiller-Baudry, M.; Sergent, M.; Chevrel, R. *Mater. Res. Bull.* **1991,** *26,* 519.

(6) Hilsenbeck, S. J.; Young, V. G.; McCarley, R. E. *Inorg. Chem.* **1994,** *33,* 1822.

(7) (a) McCarley, R. E.; Laughlin, S. K.; Spink, D. A.; Hur, N. *Abstracts of Papers*; 3rd Chemical Congress of North America, Toronto, Ontario, Canada, 1988; American Chemical Society: Washington, DC, 1988. (b) Zhang, X.; Hur, N.; Spink, D. A.; Michel, J. B.; Laughlin, S. K.; McCarley, R. E. Manuscript in preparation.

(8) (a) Saito, T.; Yamamoto, N.; Yamagata, T.; Imoto, H. *J. Am. Chem. Soc.* **1988,** *110,* 1646. (b) Saito, T.; Yamamoto, N.; Nagase, T.; Tsuboi, T.; Kobayashi, K.; Yamagata, T.; Imoto, H.; Unoura, K. *Inorg. Chem.* **1990,** *29,* 764. (c) Saito, T.; Yoshikawa, A.; Yamagato, T.; Imoto, H.; Unoura, K. *Inorg. Chem.* **1989,** *28,* 3588.

(9) Spink, D. A. Ph.D. Dissertation, Iowa State University, Ames, IA, 1989.

(10) Zhang, X.; McCarley, R. E. *Inorg. Chem.*, submitted.

0897-4756/95/2807-0499$09.00/0

ethylphosphine adduct, partial deligation was found by using phosphine acceptors like $Co_2(CO)_8$, $Mo(CO)_6$, or CuCl. Thermal deligation below 350 °C for the tungsten pyridine adduct resulted in partial pyridine removal, while heating to 640 °C caused disproportionation to tungsten and tungsten disulfide. These results indicated that more weakly ligated adducts should be studied if complete deligation is to be reached.

Furthermore, thermal deligation results in the formation of amorphous materials. In a previous paper,[6] the spectroscopic techniques of Raman and XPS have indicated the potential for answering whether the Mo_6S_8 cluster unit is retained upon thermolysis. Likewise, the technique of EXAFS has become a more prominent tool in the characterization of amorphous materials.[11] Relevant uses of EXAFS include the study of amorphous molybdenum trisulfides[12] and an alumina-supported copper Chevrel phase.[13] Yet, only a few other examples are known for EXAFS of Chevrel phases,[14] and none have examined the structural changes at lower temperatures leading toward the Chevrel phase materials.

The present paper describes the deligation of several molybdenum N-ligated cluster complexes in an attempt to produce the metastable Mo_6S_8 Chevrel phase compound, and an EXAFS study of the resulting products.

Experimental Section

Materials. The reagents and products are air and moisture sensitive. Therefore, all manipulations were performed by the use of an inert-atmosphere drybox, a high-vacuum manifold, and Schlenk techniques, unless otherwise stated. The $Mo_6S_8L_6$ cluster complexes $Mo_6S_8(PrNH_2)_{6-x}$, $Mo_6S_8(pyrr)_6$, and $Mo_6S_8(pip)_6$·7pip were synthesized as reported previously.[6] The following materials were prepared and used as model compounds for EXAFS analysis. MoS_2 (Cerac, 99%) was used as purchased. Mo_6S_8 was prepared by the delithiation of $Li_xMo_6S_8$.[15] Crystalline $Mo_6S_8(tht)_6$ was prepared by the reaction of the propylamine adduct ($Mo_6S_8(PrNH_2)_{6-x}$) with neat tetrahydrothiophene (tht) at reflux temperatures for 1 day. By the slow evaporation of the resulting filtrate, the crystalline product was obtained.[7,9] Powder X-ray diffraction data for these model compounds agree with those reported in the literature.

Physical Measurements. Infrared spectra (4000–200 cm^{-1}) were recorded with a Bomem MB-102 Fourier transform infrared spectrometer equipped with CsI optics. Samples were prepared as Nujol mulls and mounted between CsI windows. Raman spectra were obtained with a Spex Triplemate spectrometer with a PARC intensified SiPD detector cooled to −40 °C. The excitation source was a Coherent Ar^+ 200 series laser at the wavelength of 514.5 nm and the scattered radiation was collected in a backscattering geometry. The laser power at the sample was approximately 20 mW, and the integration time was 200 s. The Raman spectra were obtained at room temperature from solid samples packed in capillary tubes. XP spectra were collected with Physical Electronics Industries 5500 multitechnique surface analysis system, and the binding energies were calibrated with C 1s binding energy (BE) of 284.6 eV. Thermal analysis curves were obtained with a Seiko TG/DTA 300. Under flowing argon gas (100 cm^3/min), the samples were heated (10 °C/min) to 600 °C. Powder X-ray diffraction data were obtained with a Philips ADP3520 $\theta-2\theta$ diffractometer using Cu Kα radiation. The air-sensitive samples were loaded into a specially designed sample holder and sealed while in the drybox.[16] ^1H NMR spectra were collected in deuterated benzene on a Nicolet NT-300 MHz instrument.

Chemical Analyses. Molybdenum was determined gravimetrically as the 8-hydroxyquinolate.[17] Chlorine was determined by potentiometric titration with a standardized silver nitrate solution. Additional microanalyses for carbon, hydrogen, and nitrogen were obtained from Oneida Research Services.[18]

Thermal Deligation. Similar reaction conditions were employed for all thermolysis reactions. In a typical preparation, the sample was placed in a Pyrex ampule with joints for connection to the vacuum manifold. The ampule was then furnace heated to the desired temperature under dynamic vacuum at 10^{-4} Torr. The propylamine, pyrrolidine, and piperidine adducts were studied by this method. The temperatures were varied from 100 to 500 °C and the reaction materials were usually held at the desired temperature for a period of 1–2 days. Infrared spectra were always collected. Depending upon the product, X-ray powder diffraction data, elemental analyses, and other spectral data (Raman and XPS) were also obtained.

EXAFS Sample Preparation. $Mo_6S_8(PrNH_2)_{6-x}$ samples were each prepared by vacuum thermolysis for 8 h at a particular temperature within the range 100–500 °C. For brevity, the thermolysis products of the propylamine adduct will be indicated as **1** for 100 °C heating, **2** for 200 °C, **3** for 300 °C, **4** for 400 °C, and **5** for 500 °C heating. After thermolysis, spectral data were collected and elemental analyses were determined. On the basis of Mo analyses, the approximate formulations for the resulting products ($PrNH_2$/Mo_6 unit) were found as follows: **1**, 5.4; **2**, 2.7; **3**, 2.1; **4**, 1.6; **5**, 1.4 "$PrNH_2$" ligands.

These samples and the model compounds (MoS_2, Mo_6S_8, $Mo_6S_8(tht)_6$) were individually ground to a particle size of less than 200 mesh, while in an inert-atmosphere drybox. Pressed pellets of various sample thicknesses were prepared and placed between strips of cellophane tape in aluminum sample holders. All samples were kept under an argon atmosphere until the recording of the absorption spectra. The short-term stability of these samples was quite adequate; however, noticeable oxygen contamination resulted from air-exposure of the unheated $Mo_6S_8(PrNH_2)_{6-x}$ sample while attempting to reduce the sample thickness. Consequently, this sample was not included in the results reported here.

Data Collection. The X-ray absorption spectra were recorded in the transmission mode at the Cornell High Energy Synchrotron Source (CHESS) on beam-line C2 under typical beam conditions of 5.2 GeV and 40–70 mA. The K absorption edge of Mo was studied using a channel-cut Si (220) double-crystal monochromator detuned by 50% to avoid the effects of higher harmonics present in the X-ray beam. Energy calibration was performed with Mo metal foil by assigning the inflection point in the absorption edge as 20 000 eV. Measurements were obtained in three energy regions using a step size of 10 eV prior to the edge zone, 2 eV over the edge region, and 3 eV after this region. An 8 cm long argon-filled ionization chamber was used to measure the incident X-ray flux, while a sealed xenon chamber was utilized for the transmitted flux. For each sample, at least two spectra were obtained.

(11) Bertagnolli, H.; Ertel, T. S. *Angew. Chem., Int. Ed. Engl.* **1994**, *33*, 45.

(12) (a) Cramer, S. P.; Liang, K. S.; Jacobson, A. J.; Chang, C. H.; Chianelli, R. R. *Inorg. Chem.* **1984**, *23*, 1215. (b) Scott, R. A.; Jacobson, A. J.; Chianelli, R. R.; Pan, W.-H.; Stiefel, E. I.; Hodgson, K. O.; Cramer, S. P. *Inorg. Chem.* **1986**, *25*, 1461.

(13) Rabiller-Baudry, M.; Sergent, M.; Chevrel, R.; Prouzet, E.; Dexpert, H. *Eur. J. Solid State Inorg. Chem.* **1992**, *29*, 593.

(14) (a) Guenzburger, D.; Ellis, D. E.; Montano, P. A.; Shenoy, G. K.; Malik, S. K.; Hinks, D. G.; Vaishnava, P.; Kimball, C. W. *Phys. Rev. B* **1985**, *32*, 4398. (b) Vaishnava, P. P.; Kimball, C. W.; Matykiewicz, J. L.; Fradin, F. Y.; Shenoy, G. K.; Montano, P. A. *Phys. Rev. B* **1986**, *34*, 4599. (c) Holtman, D. A.; Teo, B. K.; Tarascon, J. M.; Averill, B. A. *Inorg. Chem.* **1987**, *26*, 1669.

(15) Behlok, R. J.; Kullberg, M. L.; Robinson, W. R. *Proceedings of the 4th International Conference on the Chemistry and Uses of Molybdenum*, Barry, H. F., Mitchell, P. C. H., Eds.; Climax Molybdenum Co.: Ann Arbor, MI, 1982; p 23.

(16) Design of the air-sensitive sample holder is given in: Close, M. R. Ph.D. Dissertation, Iowa State University, Ames, IA, 1992.

(17) Elwell, W. T.; Wood, D. F. *Analytical Chemistry of Molybdenum and Tungsten*; Pergamon Press: New York, 1971; p 41.

(18) Oneida Research Services, Inc., Whitesboro, NY.

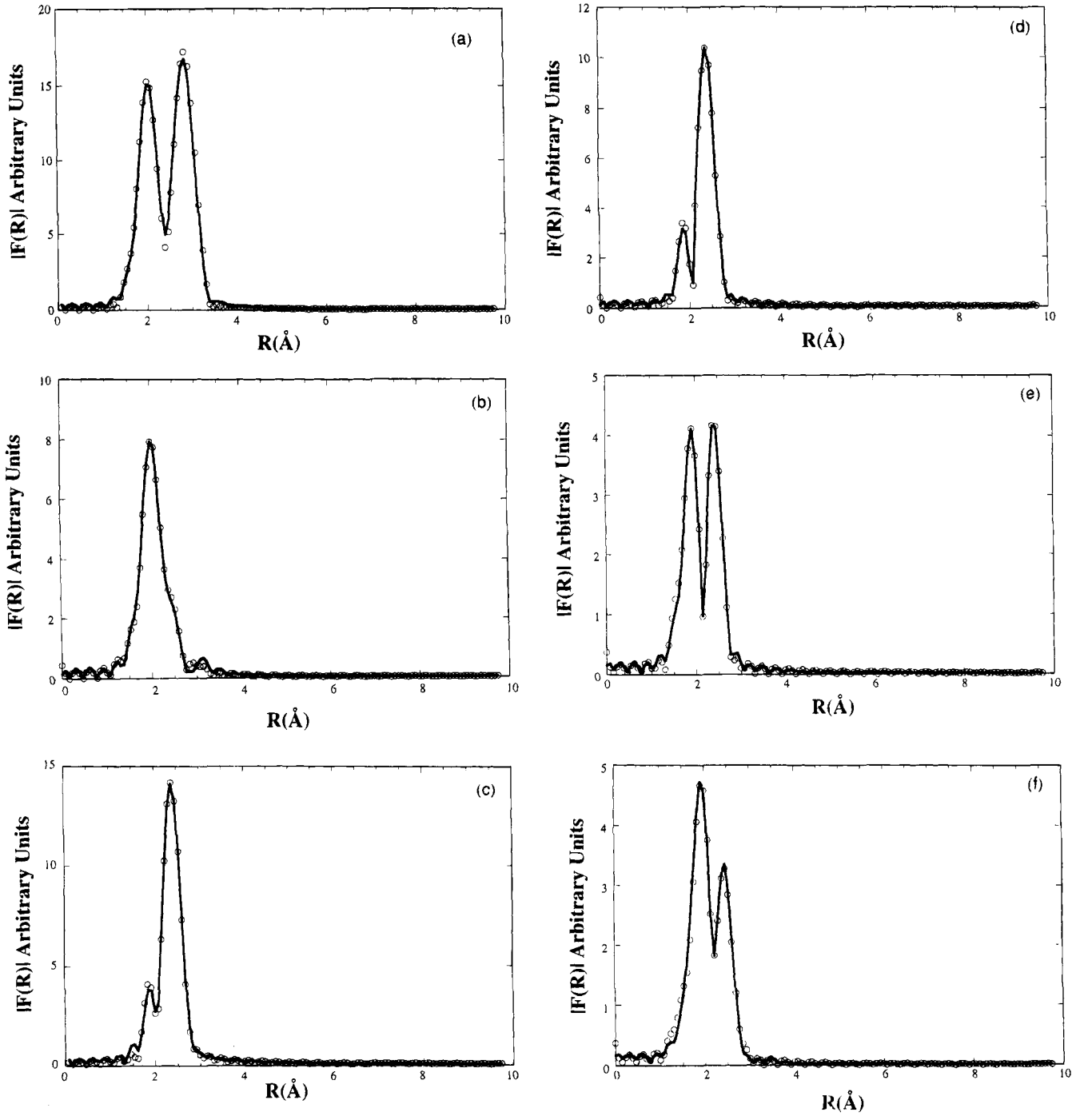

Figure 2. Fourier transformed EXAFS data (dotted curve) and best-fit results of curve fitting (solid curve) for (a) MoS_2, (b) Mo_6S_8, (c) $Mo_6S_8(tht)_6$, and thermal deligation of $Mo_6S_8(PrNH_2)_{6-x}$ at (d) 100, (e) 200, and (f) 500 °C.

Data Analysis. The EXAFS data were reduced and analyzed using standard techniques with programs developed by Michalowicz[19] and the University of Washington.[20] The spectra were subjected to background removal and normalization using standard procedures—linear preedge function, removal of background curvature using a high-order (5th–6th) polynomial or by spline polynomial with division of the absorption spectrum into zones selected manually—and were selected to give the best signal-to-noise ratio and minimum mean standard deviation. For all spectra, E_0 was chosen initially as the edge energy and refined during curve fitting of the data as described below.

After removal of the smooth atomic absorption contribution from the data and normalization to the step height, the EXAFS oscillations were Fourier transformed (Figure 2). The Fourier transformation was carried out over the range 4–14 $Å^{-1}$ for all data using a Hanning window function and k^3 weighting. The first two peaks in the transform were isolated and then back-transformed to k space. The filtered oscillations were then subjected to a nonlinear least-squares fit to a parameterized EXAFS expression using two (three where required) shells of Mo and S scatterers. The phase shift and amplitude functions for the model compounds were calculated from the stated programs.[19] These values were then adopted for the deligation samples. Parameters to account for the inelastic mean free Debye–Waller factor, overall scale factor, and photoelectron mean free path were determined from fits to model compounds and fixed for the samples in question.

(19) Michalowicz, A. *Logiciels pour la Chimie*, Société Française de Chimie, Eds.; Paris, 1991; p 102–103.

(20) MACEXAFS Version 3.1, University of Washington EXAFS Analysis Package.

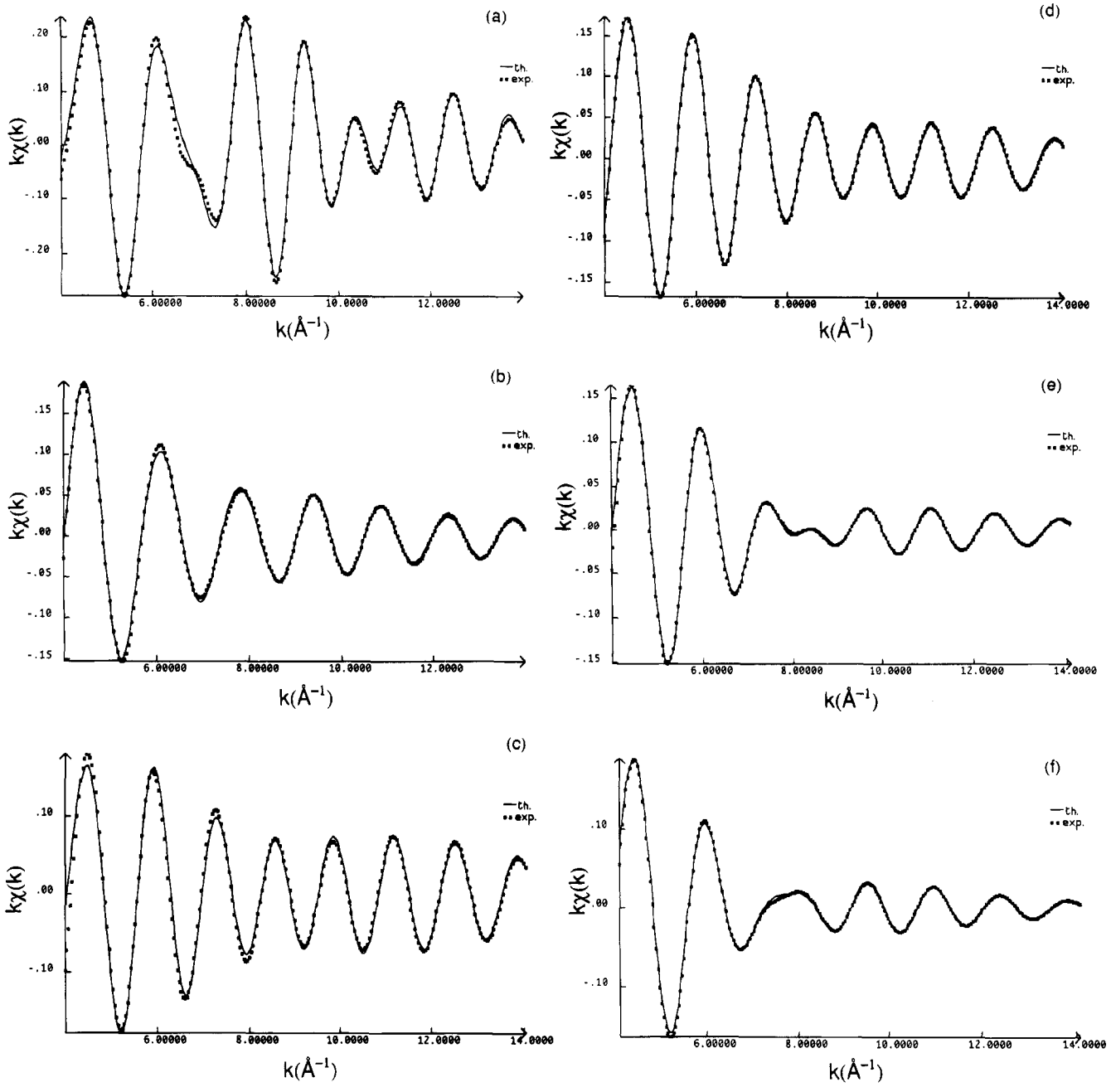

Figure 3. Filtered data (dotted curve) and best-fit results of curve fitting (solid curve) for EXAFS of (a) MoS_2, (b) Mo_6S_8, (c) $Mo_6S_8(tht)_6$, and the thermal deligation of $Mo_6S_8(PrNH_2)_{6-x}$ at (d) 100, (e) 200, and (f) 500 °C.

Quantitative analysis was performed by systematically varying the coordination number N_i (fixed at crystallographic values for the model compounds), the Debye–Waller factor σ_i, and the distance of the ith shell of atoms from the absorber atom R_i. The resulting average spectra $\chi(k)$ vs k after filtering and curve fitting are shown in Figure 3.

Results and Discussion

Thermal Deligation. The method of vacuum thermolysis is reported here as the first route explored for the cluster complexes. On the basis of bond distance data, the terminal molybdenum–nitrogen bond of the adduct is weaker than the corresponding molybdenum–sulfur bonds in the Chevrel phase structure.[6] Thus, cleavage of the Mo–N bond may be facilitated by the formation of the Mo–S bonds which knit the cluster units together in the network structure of the binary Mo_6S_8. This ideal process is indicated by eq 1. However,

$$Mo_6S_8L_6 \rightarrow [(Mo_6S_2S_{6/2})S_{6/2}] + 6L \quad (1)$$

rather than clean dissociation, ligand fragmentation is also a possible outcome. Fragmentation and incomplete removal of the ligand would result in the random blocking of intercluster linkages and produce a disordered material. As a precautionary measure, deligation temperatures were limited to about 500 °C because the binary Mo_6S_8 phase has been reported to be thermally unstable; above this temperature, Mo_6S_8 successively undergoes a phase transformation and decomposition to molybdenum and molybdenum disulfide.[21,22] A recent report claims that, after phase transformation ($\alpha \rightarrow \beta$), Mo_6S_8 is stable under H_2 flow or in vacuo to 900 °C;

(21) Chevrel, R.; Sergent, M.; Prigent, J. *Mater. Res. Bull.* **1974**, *9*, 1487.
(22) Schöllhorn, R.; Kümpers, M.; Plorin, D. *J. Less-Common Met.* **1978**, *58*, 55.

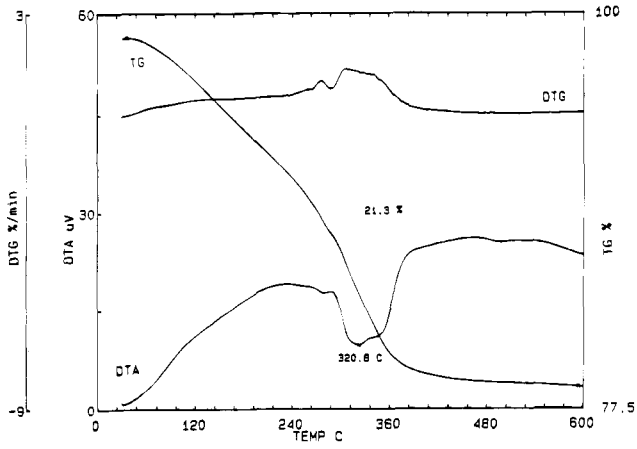

Figure 4. Thermogravimetric analysis of $Mo_6S_8(PrNH_2)_{6-x}$ complex under an argon atmosphere.

however, the XRD pattern indicates the presence of MoS_2 and Mo decomposition products.[23]

Propylamine Complex. The first step in understanding the thermal deligation process was to study pyrolysis via TG/DTA. The resulting TG/DTA curve for the propylamine complex is shown in Figure 4. As observed in this figure, weight loss occurred quite quickly (T_{onset} ~ 50 °C) and showed a steady weight loss to almost 400 °C before levelling off. The observed weight loss of 21.3% corresponded to the removal of about four propylamine ligands, and this black product exhibited a featureless infrared spectrum.

Deligation *in vacuo* should result in more complete ligand removal since the reactions proceed for longer times under dynamic vacuum as compared to the TG/DTA study. Therefore a lower temperature of 250 °C was initially chosen and resulted in the formation of a shiny, gray-black amorphous solid. The far-infrared spectrum of this product exhibited a very weak and broad Mo–S peak centered about 386 cm^{-1}. Also, the mid-IR region was completely devoid of propylamine bands. The Mo analyses on this material (62.13% Mo) indicated lower content than that calculated for Mo_6S_8 (69.18%). XPS binding energies corroborated that this material contained the cluster unit and that MoS_2 was not present.[6]

Further heating of the propylamine adduct to 350 °C again resulted in the formation of a shiny, yet amorphous, gray-black solid. The far-infrared spectrum became featureless as the weak Mo–S band was lost among the background noise. Molybdenum analyses (67.99% Mo) on this product indicated that some organic residue must be present. This result might be understood as arising from some fragmentation of the propylamine ligand, because, during pyrolysis, a noticeable pressure increase on the vacuum line at about 300 °C was observed. This increase in pressure could be due only to volatile gases, such as methane or hydrogen arising from propylamine fragmentation, which would not condense in the liquid nitrogen trap.

Raman spectra for the initial propylamine cluster complex and the product of deligation at 500 °C are shown (Figure 5) in comparison to the crystalline Chevrel phase Mo_6S_8. The presence of the broad band

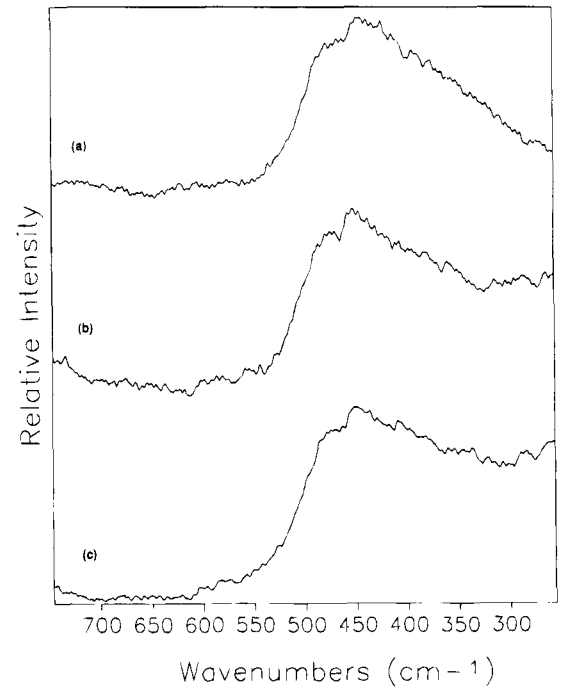

Figure 5. Raman spectra of (a) $Mo_6S_8(PrNH_2)_{6-x}$ complex, (b) the product of deligation at 500 °C under dynamic vacuum, and (c) crystalline Mo_6S_8. The broad peaks are centered at about 448–450 cm^{-1}.

centered at 448 cm^{-1} in these spectra indicates that the Mo_6S_8 cluster unit has been retained after thermolysis. Likewise, all other deligation products from lower temperature thermolysis resulted in identical Raman spectra to those shown in Figure 5.

Pyrrolidine Complex. The TG/DTA curve for the pyrrolidine adduct exhibits initial sample stability (25–100 °C) before undergoing a strong weight loss (~20%) over the region 120–300 °C, and then a slight, but steady, loss through the rest of the experiment. The total weight loss of 23.6% corresponds to 4.4 pyrrolidines removed. The resulting product was an amorphous black powder.

Thermal deligation was also explored in vacuo at 350 and 450 °C. A black, amorphous powder was obtained upon heating to 350 °C. The far-infrared spectrum of this solid showed a very weak, broad Mo–S band centered about 395 cm^{-1}. Further heating of the same material to 450 °C also resulted in a black, amorphous powder. The molybdenum content of the sample heated to 450 °C, 63.91%, was again lower than the calculated value for Mo_6S_8 (69.18% Mo). This result also indicates the presence of some organic residue.

Piperidine Complex. The TG/DTA curve of the crystalline adduct $Mo_6S_8(pip)_6 \cdot 7pip$ shows an almost immediate weight loss as expected for a compound containing seven lattice piperidines per cluster unit. This sharp loss over the region 30–100 °C of 25.7% corresponds to about six molecules of piperidine. A lower weight loss of 6.7% (approximately 1.5 pip) is found from 100 to 160 °C, and then it is continuous over the rest of the temperature range. The total weight loss of 56.5% corresponds to all 13 piperidines being removed. The resulting product was a brown/black powder.

On the basis of the large initial loss of piperidine, heating of the adduct at 100 °C under dynamic vacuum was explored to prepare an intermediate freed of the

(23) Rabiller, P.; Rabiller-Baudry, M.; Even-Boudjada, S.; Burel, L.; Chevrel, R.; Sergent, M.; Decroux, M.; Cors, J.; Maufras, J. L. *Mater. Res. Bull.* **1994**, *29*, 567.

lattice piperidine. The resulting product was an amorphous brown powder whose infrared spectrum showed the presence of coordinated piperidine and a shifting of the Mo–S peak from 382 to 387 cm^{-1}. The material was not as soluble as before heating, but the NMR spectrum in deuterated benzene showed bands identifiable as both coordinated and free (lattice) piperidine.[6] The bands for free piperidine were much weaker than previously observed; however, their presence indicated incomplete removal of the lattice piperidine. This heated material was redissolved in neat piperidine, and the crystalline complex was grown from the resulting pinkish-red solution.

Heating of the piperidine adduct to 300 °C was also explored. The thermolysis product was found to be an amorphous black powder. This material did not dissolve in either neat piperidine or benzene, which indicated that the thermolysis product was sufficiently crosslinked to render it insoluble. Both Raman and XPS confirmed that the Mo_6S_8 unit remained. Likewise, the resulting Mo analyses (62.03%) indicate the presence of some organic residue.

EXAFS Study and Structural Characterization. Samples for this study were prepared by deligation of the propylamine adduct via thermolysis in vacuo over the range 100–500 °C. In all cases, the resulting products were amorphous, virtually insoluble solids. Previous study of the crystalline and amorphous $Mo_6S_8L_6$ cluster complexes indicated that the spectroscopic techniques of Raman and XPS were reasonable tools to examine whether the Mo_6S_8 cluster unit is retained.[6] The observed binding energies for the deligation products all fall reasonably close to one another [Mo $3d_{5/2}$, 227.4–227.6; Mo $3d_{3/2}$, 230.6–230.8; S 2s, 225.3–225.5; S 2p (broad), 161.4–161.6 eV] and to those of the starting propylamine adduct. Furthermore, the Mo 3d values are similar to those reported for the binary Chevrel phase Mo_6S_8.[24] The Raman spectra all exhibit one broad peak centered about 448–450 cm^{-1} (as previously shown in Figure 5).

Yet, these spectroscopic techniques do not unambiguously prove that the Mo_6S_8 cluster unit is retained or provide evidence about what is occurring during the deligation process. Therefore, an EXAFS study was undertaken to gain information about the $PrNH_2$ adduct and the changes in the Mo atom environment of the cluster during deligation.

Model Compounds. The results of nonlinear least-squares fitting on these compounds (Table 1) are consistent with bond distances derived from reported crystallographic structure determinations. All of the experimental bond distances from EXAFS are within 0.03 Å of the reported values. Likewise, the Debye–Waller factors are quite consistent over the range 0.06–0.08 Å for both the Mo and S shells of all model compounds.

MoS_2. The FT spectrum (Figure 2a) exhibits two peaks arising from the six first sulfur neighbors of Mo (d(Mo–S) = 2.42 Å) and the six neighboring Mo atoms (d(Mo–Mo) = 3.16 Å).[25]

Mo_6S_8. The binary Chevrel phase Mo_6S_8 shows only a single peak in the FT spectrum (Figure 2b). This result was previously noted for $Cu_4Mo_6S_8$, and the presence of only a single broad peak was confirmed by simulation from theoretical data.[13] Elongation along the 3-fold axis leads to a distortion of the cluster units in Mo_6S_8 and requires multiple shells to fit the data. These four shells are composed of one sulfur shell arising from four triply-bridging sulfur atoms in the cluster unit and one sulfur atom from a neighboring unit via an intercluster S–Mo bond, and three molybdenum shells arising from (1) the two closer symmetry-equivalent Mo atoms within the Mo_3 triangle caused by the distortion, (2) two Mo–Mo bonds to the nearest neighbor atoms in the adjoining Mo_3 triangle (Δ–Δ), and (3) the final intercluster Mo–Mo bond.[21]

Table 1. Comparison of Structural Parameters Derived from EXAFS Mo-Edge Data[a]

	shell	N	R_{EXAFS}, Å[b]	R_{cryst}, Å	σ, Å	ΔE, eV
MoS_2	S	6	2.42	2.42	0.06	4.7
	Mo	6	3.16	3.16	0.06	−3.1
Mo_6S_8	S	5	2.46	2.44	0.08	4.0
	Mo	2	2.73	2.70	0.06	0.7
	Mo	2	2.89	2.86		
	Mo	1	3.06	3.08		
$Mo_6S_8(tht)_6$	S	4	2.46	2.43	0.06	3.2
	S	1	2.61	2.58		
	Mo	4	2.65	2.64	0.06	−2.3
100	S	4	2.47		0.06	4.4
	Mo	4	2.64		0.07	−4.9
	N	1[c]	2.31		0.06	−10.5
200	S	4	2.43		0.07	2.4
	S	1[c]	2.64			
	Mo	2	2.61		0.09	−5.2
	Mo	2	2.67			
500	S	4	2.43		0.07	2.8
	S	1[c]	2.57			
	Mo	2	2.62		0.09	−6.6
	Mo	2	2.71			

[a] N, number of atoms in the shell; R, distance from Mo absorber; σ, Debye–Waller factor; ΔE, shift in energy origin. [b] Error in the experimental bond distances based on fitting is on the order of ±0.03 Å. [c] Error in the number of atoms based on fitting is on the order of ±0.5.

$Mo_6S_8(tht)_6$. The S-ligated cluster complex was used as a model for the molecular $Mo_6S_8L_6$ adducts because of its stability and absence of excess ligand acting as solvent of crystallization (as in the crystalline pyrrolidine and piperidine adducts). Ideally, the propylamine complex would be used; however, this material can only be prepared in a slightly ligand-deficient form. The FT spectrum for the tht adduct (Figure 2c) exhibits two peaks arising mainly from the Mo–S and Mo–Mo shells. An attempt to fit the data without the S-ligand (tht) shell resulted in an underestimation for the second peak. Nonlinear least-squares fitting with three shells produced good agreement with the crystallographic data.[9]

Structural Characterization. As shown in Figure 2, the thermal deligation products for $Mo_6S_8(PrNH_2)_{6-x}$ show distinct differences between the 100 °C sample (**1**) and samples from thermolysis at higher temperatures (**2**, **5**). However, the FT spectrum for **1** (Figure 2d) is virtually identical to that for the crystalline tht adduct (Figure 2c). Although the data are not reported due to problems with oxygen contamination, the spectrum of the unheated $PrNH_2$ complex is also very similar to those of **1** and tht. These observations are in agreement with other similarities between **1** and $Mo_6S_8(PrNH_2)_{6-x}$. Both are soluble in neat *n*-propylamine. The infrared spectrum for **1** is identical to that of the unheated

(24) Yashonath, S.; Hegde, M. S.; Sarode, P. R.; Rao, C. N. R.; Umarji, A. M.; Subba Rao, G. V. *Solid State Commun.* **1981**, *37*, 325.
(25) Dickinson, R. G.; Pauling, L. *J. Am. Chem. Soc.* **1923**, *45*, 1466.

$PrNH_2$ adduct in that both exhibit characteristic bands for $PrNH_2$ and the strong Mo–S stretching mode at 381 cm^{-1}. Elemental analyses for **1** also show slightly less than six ligands per cluster unit, almost the same as in the unheated material. The derived structure parameters (Table 1) are also indicative of molecular $Mo_6S_8L_6$ cluster complexes. The Mo–S distance of 2.47 Å, Mo–Mo distance of 2.65 Å, and Mo–N distance of 2.31 Å are identical (within experimental error) to the N-ligated cluster complexes reported previously.[6] These results indicate that heating to 100 °C, even with slight loss of $PrNH_2$ ligands, does not significantly change the environment of the isolated Mo_6S_8 cluster unit. An attempt to fit the EXAFS data with a second S shell (arising from close approach of a neighboring cluster) exhibited unreasonable fit results and lent further support for the existence of isolated cluster units in **1**.

As noted above, distinct differences are found as the thermolysis temperature is raised to 200 °C. This change can be readily observed in both the FT spectra (Figures 2d for **1** and 2e for **2**) and the resulting EXAFS back-transformed spectra (Figures 3d and 3e, respectively). Elemental analyses show a large amount of propylamine loss such that there are less than three $PrNH_2$ ligands/Mo_6 unit, and that **2** is no longer soluble in neat *n*-propylamine. The IR spectrum for **2** still exhibits very weak $PrNH_2$ bands and a very broadened Mo–S band centered at 381 cm^{-1}. These physical results indicate that upon removal of $PrNH_2$, the cluster units are becoming interlinked via Mo–S intercluster bonding. This process would be expected to occur in a rather random manner considering the low temperature of the reaction relative to removal of propylamine (Figure 4). Likewise, the presence of residual $PrNH_2$ ligands should block some of the potential interlinkage sites and lead to a rather disordered arrangement for intercluster bonding.

The derived structure parameters for **2** (Table 1) indicate a phase intermediate between that of the molecular cluster unit and crystalline Mo_6S_8. As expected, the results of fitting showed the presence of a second S shell at a long distance of 2.64 Å arising from the advent of intercluster S–Mo bonding. The observed number of atoms for this S shell was higher than expected and thus is inconsistent with the presence of some remaining $PrNH_2$ as detected by IR and elemental analyses. However, attempts to fit the data with an additional N shell exhibited unreasonable results, which indicated that the system disorder produces an insensitivity to this amount of nitrogen relative to sulfur. Fitting of the EXAFS data with a single Mo shell resulted in unreasonably large Debye–Waller factors and prompted its splitting into two equal Mo shells. In a fashion similar to that for Mo_6S_8, a slight trigonal elongation of the Mo_6 unit is observed such that shorter distances (2.61 Å) arise within the Mo_3 triangle and slightly longer distances (2.67 Å) arise between the triangles. The distortion for **2** is not as drastic as observed in Mo_6S_8, most likely due to the lack of complete Mo–S intercluster bonding.

EXAFS data for the 300 °C (**3**) and 400 °C (**4**) samples showed little difference from the 500 °C sample (**5**), thus the former will not be discussed in any detail. As previously noted, the elemental analyses indicated subsequent removal of propylamine (or organics). Furthermore, these samples did not exhibit any solubility in *n*-propylamine. The mid-IR spectra for **3** and **4** are devoid of $PrNH_2$ peaks, while in the far-IR spectra a very weak, broad Mo–S stretching band was detected at 392 cm^{-1} for **3**, but this was completely absent for **4**.

Of initial significance, the EXAFS spectrum for **5** (Figure 3f) shows no indication of cluster decomposition and formation of MoS_2 (Figure 3a, for comparison). This result supports the conclusion drawn from the Raman and XPS data that the Mo_6S_8 cluster is stable at this thermolysis temperature. Elemental analyses still indicate the presence of organics (4.00% C, <0.5% H, 0.95% N) which are probably surface residue arising from fragmentation of $PrNH_2$ at temperatures above 300 °C, as previously noted in the $PrNH_2$ deligation studies. Comparison of the EXAFS back-transformed spectra for **5** (Figure 3f) to Mo_6S_8 (Figure 3b) shows strong similarities between the spectra, except for the 7.0–8.5 $Å^{-1}$ region where a broad, unresolved oscillation is noted for **5** in contrast to a sharper peak for the crystalline Mo_6S_8.

As observed for **2**, fitting of the 500 °C data involved the addition of a second S shell. At this deligation temperature, interlinkage of clusters through Mo–S bonds should be prevalent and probably more ordered than would be expected at 200 °C. As noted in Table 1, the second S shell produces an intercluster Mo–S bond with an average distance of 2.56 Å. This result is similar to the value found for terminal sulfur bonding in the tht adduct (2.58 Å), while being much longer than what is observed for Mo_6S_8 with full cluster interlinking (2.44 Å). The results of the fitting (Table 1) indicate that there is a more noticeable distortion of the cluster unit. As previously noted for **2**, the observed Mo–Mo bond distances reflect a smaller distortion than that present in crystalline Mo_6S_8.

Deligation Process. Upon thermolysis, the $Mo_6S_8L_6$ isolated cluster units exhibit loss of ligand which can lead to the formation of a vacant site and then subsequent interlinkage of cluster units via weak Mo–S bonds. Heating at 100 °C results in a slightly ligand-deficient product which shows no evidence of forming interlinkages. The large number of $PrNH_2$ ligands effectively block close-enough approaches between the vacant sites and thus prevent the formation of intercluster bonds. Yet, by 200 °C the loss of ligand is enough to allow close approach and subsequent formation of weak intercluster Mo–S bonds. This bonding should be predominantly of the single bridge type (Mo–S–Mo) owing to the steric problems arising from the presence of some remaining ligand and the rather haphazard manner in which the clusters are being interlinked. As the temperature is increased to 500 °C, further change occurs with a slight shortening of the average Mo–S intercluster bonds and likewise further slight distortion of the Mo_6 units. The conditions are not yet suitable for the complete formation of double bridges between the clusters which produces the longer intercluster Mo–Mo bonds characteristic of crystalline Mo_6S_8.

Conclusions

This paper describes the thermal deligation studies on several N-ligated $Mo_6S_8L_6$ cluster complexes and the characterization of the resulting products. Thermal

analysis by TG/DTA provided initial temperature ranges where significant ligand removal was occurring; however, the upper heating limit was fixed at about 500 °C since Mo_6S_8 was reported to disproportionate to Mo and MoS_2 near this temperature. Direct heating under dynamic vacuum for all the complexes resulted in significant, yet incomplete deligation, as evidenced by low molybdenum analyses and traces of organic residues from C, H, N analyses. It was reasoned that some ligand fragmentation occurs at temperatures above 300 °C, where noncondensable gases become evident in the evolved products, e.g., hydrogen and methane.

Thermal deligation of these $Mo_6S_8L_6$ cluster complexes resulted in the formation of amorphous materials which became challenges to characterize. Normal spectroscopic techniques like NMR or IR were of little help since the materials were insoluble and showed featureless IR spectra upon thermolysis. Therefore, other spectroscopic tools were employed to study and characterize the resulting products. Raman, XPS, and EXAFS all support the retention of the Mo_6S_8 unit upon thermolysis, even to temperatures as high as 500 °C. Characteristic values for the cluster unit can be obtained for each of these techniques, which differ from the values found for the known disproportionation products—MoS_2 and Mo metal.

Furthermore, the EXAFS study provided insight into changes that are occurring to the cluster complexes as the thermal deligation proceeded. Thermolysis at temperatures of 100 °C or less resulted in little change to the $Mo_6S_8(PrNH_2)_{6-x}$ complex, while heating at 200 °C or above resulted in significant changes to the material. The higher temperatures cause greater ligand loss and consequently linkage of clusters through intercluster Mo−S bonding. The EXAFS study shows that by 500 °C a product forms which has numerous similarities to the desired Mo_6S_8 Chevrel phase. Subsequent research is being conducted to establish other deligation methods that will result in cleaner ligand removal, and thus aid in the formation of the Chevrel phase at lower temperatures.

Acknowledgment. This work was supported by the U.S. Department of Energy, Office of Basic Energy Sciences, through Ames Laboratory operated by Iowa State University under Contract No. W-7405-Eng-82. CHESS is supported by the National Science Foundation under Grant No. DMR-87-19764.

CM940395J